DESIGN AND ANALYSIS OF REACTOR CONTAINMENT OF STEEL-CONCRETE COMPOSITE LAMINATED SHELL

K. ICHIKAWA

Shimizu Construction Co., Ltd., 2-1, Takara-cho, Chuo-ku, Tokyo, Japan

O. ISOBATA

The Research Laboratory, Shimizu Construction Co., Ltd., 4-17, Etchujima-3, Koto-ku, Tokyo, Japan

S. KAWAMATA

Tohoku Institute of Technology, Sendai-shi, Japan

SUMMARY

Reinforced and prestressed concrete containments for reactors have been developed in order to avoid the difficulties of welding of steel containments encountered as their capacities have become large: growing thickness of steel shells gave rise to the requirement of stress relief at the construction sites.

However, these concrete vessels also seem to face another difficulty: the lack of shearing resistance capacity. As the design condition becomes severe, overall membrane shearing stress due to seismic horizontal force and transverse shearing stress at the shell-base junction become very high. The latter is dominant in inner pressure and thermal loading cases as the shell deformation is constrained by the base mat. These shearing stresses tend to enforce over-reinforcement of the concrete shell.

In order to improve the shearing resistance capacity of the containment vessel, while avoiding the difficulty of welding, a new scheme of containment consisting of steel-concrete laminated shell is being developed.

In the main part of a cylindrical vessel, the shell consists of two layers of thin steel plates located at the inner and outer surfaces, and a layer of concrete core into which both the steel plates are anchored. Because of the compressive and shearing resistance of the concrete core, the layers behave as a composite solid shell. Membrane forces are shared by steel plates and partly by concrete core. Bending moment is effectively resisted by the section with extreme layers of steel. Therefore, both surfaces can be designed as extremely thin plates: the inner plate, which is a load carrying member as well as a liner, can be welded without the laborious process of stress-relieving, and various jointing methods can be applied to the outer plate which is free from the need for leak tightness.

The capability of the composite layers of behaving as a unified solid shell section depends largely on the shearing rigidity of the concrete core. However, as its resisting capacity to transverse shearing force is comparatively low, a device for reducing the shearing stress at the junction to the base mat is needed. In the new scheme, this part of the cylindrical shell is divided into multiple layers of the same kind of composite shell. This device makes the stiffness of the bottom of the cylindrical shell to lateral movement minimum while maintaining the proper resistance to membrane forces. The analysis shows that the transverse shearing stress can be reduced to less than $1/\sqrt{n}$ of the ordinary case by dividing the thickness of the shell into n layers which are able to slip against each other at the contact surface.

In order to validate the feasibility and safety of this new design, the results of analysis on the basis of up-to-date design loads are presented.

The results of model tests in 1:30 scale are also reported. A series of experiments are underway regarding to ultimate strength under inner pressure and seismic horizontal forces.

Behaviour of the multiple layered shell end junction with the base slab is also investigated in this series.

1. Introduction

The design and analysis of a typical reinforced concrete containment for a 1,100MW Boilling Water Reactor is presented as an introduction for proposing the new scheme of Steel-Concrete Composite Laminated Shell Containment.

The typical containment structure consists of vertical cylinder with hemispherical dome and a flat bottom slab.

To resist the postulated high seismic forces, combination building is connected with the containment at each floor level.

For the purpose of the comparison the containment which has no connection with combination building, a free standing containment, is also designed.

Figure 1 shows an outline of a reinforced concrete containment with a combination building.

The basic dimensions, design conditions and configuration for the structures are summarized as follows:

Inside diameter : 40.0 m, Height of spring line : 43.5 m

Foundation mat thickness : 7.0 m, Wall thickness : 1.5 m, Dome thickness : 0.8 m,

Loss of coolant accident design pressure (Pa)	:	15 psi, 45 psi,
Design temperature	:	see Table 1,
Intensity of Safe Shutdown Earthquake (Ess)	:	0.45 g,
Intensity of Operation Basis Earthquake (Eo)	:	0.30 g,
Concrete compressive strength	:	240 kg/cm^2
Reinforcing steel yield stress	:	2400 kg/cm^2
Load combinations	:	see Table 2.

With reference to Figure 1, the positions from the top of the containment to the base are represented by A, B, C, D and E, and stresses at each position are shown in Tables 3 and 4.

Meridional tension N1 (T/M), radial moment M1 (TM/M), circumferential tension N2 (T/M), circumferential moment M2 (TM/M), transverse shearing force Q(T/M), and in-plane shearing force N(T/M) are tabulated by the thermal conditions and load combinations.

Effects of two different thermal conditions are : (1) average temperature change Ta, and (2) thermal difference change Tg which are shown respectively in Table 3.

The maximum value of the resultant of these thermal effects at each position would govern the design of containment wall section.

Table 4 shows forces and moments at each position, which result from the different loading conditions.

The tensile fiber stresses at the outer surface of the concrete wall which are obtained by the elastic analysis of uncracked section are shown in Figure 3.

The resultants of tensile stresses caused by the stipulated load combinations at each position are graphically expressed in this Figure.

Figure 4 shows the stress levels induced by the stipulated loads and load combinations to the wall shear at the junction with the base mat.

The design method of this reinforced concrete containment has followed ASME section III division 2.

The conclusions of these design studies are summarized as follows.

1) As the reinforced concrete containment has a large section, the compressive capacity is comparatively high, and in many cases, the design of the reinforced concrete section is only governed by the amount of tensile reinforcing steel.

2) Effects or sensibilities of each load are different by the positions on the containment as shown in Figure 3.

At the dome part, effects of inner pressure load is dominant and the load combination of Abnormal condition with 1.5 pa has governed the design of the reinforced concrete sections.

For the cylindrical wall part, as the postulated seismicity is too high, so the critical load combination is the extreme/Abnormal condition.

Radial shear stress at the cylindrical wall junction with the base slab is governed mostly by the inner pressure and thermal expansion of the wall as shown in Figure 4.

3) With reference to Figure 3, the thermal effect has dominated in the resultant of load combinations because of using elastic analysis. As thermal stresses are self limiting, creep and developing cracks causes the reduction of restrained forces, so the thermal stresses are becoming lower but it is difficult to evaluate it accurately.

Three types of thermal effects are considered: the average temperature change Ta results in a dominant effect to the radial shear force at the base of wall; the thermal difference change Tg results in a dominant effect to the value of bending moment in the dome and cylindrical wall; effect of liner expansion, which is assumed as the same effects of inner pressure, should be evaluated when the design pressure Pa is postulated extremely low.

4) It is natural to predict that many cracks will exist in reinforced concrete structures. These inherent cracks cause decreasing thermal stresses but to evaluate the effect on the integrity of containment is the difficult problem.

Surface cracks of the cylindrical wall part which are caused by bending can be controlled and have little effect on the integrity of containment. But the shear cracks and tension cracks which are presumed to penetrate the full section are the problem for the integrity of containment.

5) To guarantee the integrity of the pressure boundary, special consideration should be given to the details, especially to the parts of the dome and the cylindrical wall end. From Figure 3, we can recognize the fact that the pressure capacity of the dome part is relatively low compared with the cylindrical wall part.

To use a large load factor for the design pressure Pa is recommended for containment design as it contributes to the safety of the reactor system remarkably.

The new concept of Steel-Concrete Composite Laminate Shell dome and cylindrical wall is proposed to avoid many of the problems mentioned above and is expected to eliminate the requirement of heavy shear reinforcement at the wall base.

2. Design Concept of Steel-Concrete Composite Laminated Shell Containment

The main purpose of proposing the new scheme of the containment shell is:

1) to increase the ultimate strength of the containment, especially the in-plane and transverse shearing stress capacity, and

2) to facilitate the fabrication and construction of the structure.

As shown in Figure 6, the containment wall has two steel membranes, 16 mm in thickness, on both surfaces, which are anchored to and sandwich a concrete core.

Both steel membranes behave as load carrying facing members of the composite shell.

Though the inner membrane, being liner at the same time, must be fabricated by site-welding, stress relieving is not required because of its extremely small thickness. The outer membrane is assembled from fabricated panels by the use of splices and friction bolts.

The concrete core is reinforced by a nominal amount of rebars for the purpose of crack control.

The outer membrane is elected in consecutive series of circular rings which are completed by jointing individual panels, while the concreting proceeds parallel with the lift of the height of a panel. Either ordinary poured concrete or prepact aggregate concrete may be used.

Figure 6 shows the typical wall sections for Part D in Figure 5. One set of the critical stresses for this part is

$$N_2 = 350 \text{ t/m}, \qquad M_2 = 221 \text{ t/m} \tag{1}$$

which is caused by the inner pressure and temperature change in the case of Loss of Coolant Accident. The interaction curves of the allowable in-plane force and bending moment for the designed section are shown in Figure 7. As seen in the figure, the stress level is well within the allowable limit.

Another critical stress for the same part is the in-plane shearing force accompanied by Safe Shutdown Earthquake, that is

$$N = 559 \text{ t/m} \tag{2}$$

Provided that this force is resisted only by the steel membranes, we have the following result.

$$\tau_{\theta\varphi} = 1{,}745 \text{ kg/cm}^2 < \tau_{alow} = 2{,}865 \text{ (SM50)} \tag{3}$$

For the section of cylinder-base mat junction, the critical stresses, obtained for the ordinary single-layered shell end, are

$$M_1 = 279 \text{ tm/m}, \qquad Q_1 = 147 \text{ t/m} \tag{4}$$

comming from Loss of Coolant Accident. The bending moment is within the allowable limit. The transverse shearing stresses of the concrete core become

$$\tau_{\varphi r}\text{, mean} = \frac{1{,}470 \text{ kg/m}}{180 \text{ cm}} = 8.15 \text{ kg/cm}^2 \tag{5}$$

$$\tau_{\varphi r}\text{, max} = 1.5 \times 8.15 = 12.3 \text{ kg/cm}^2$$

These values would increase depending on the assumption of the effective Young's modulus used in the thermal stress analysis (the above figures were obtained assuming E'=E/2). In order to reduce the level of transverse shearing stress, the bottom of the cylinder divided into two layers was proposed in the design as shown in Figure 5. This device will lower the bending stiffness of the shell end and make it less sensitive to the constraining effect of the base mat, while maintaining the stiffness and strength against the in-plane stresses.

In the double-layered part of the cylinder (Part E in Figure 5), where bending stresses dominate, both layers are in the condition of plate-to-plate contact and are able to slip against each other under the action of transverse shearing force. Detailed discussion on the effect of this design is to be given in the following section.

Further, the steel membranes of each layer are connected to each other by a series of thin web plates. Therefore, the concrete core is confined in the space surrounded by steel plates and has high resistance capacity against the shearing stress.

3. Characteristics of Multi-Layered End of Cylindrical Shell

According to the theory of thin elastic shells, the solution of bending of a edge-loaded infinitively long shell shown in Figure 8-a is represented by

$$w = e^{-\kappa_0 \xi} (C_1 \cos \kappa_0 \xi + C_2 \sin \kappa_0 \xi) \qquad (6)$$

where, $\xi = x/a$, $\kappa_0 = \sqrt[4]{3(1-\nu^2)}\sqrt{\frac{a}{t_0}}$, ν : Poissons ratio (7)

The boundary conditions for the fixed end of cylindrical shell subjected to inner pressure p is given as

$$w = -w^M = -\frac{a^2 p}{E t_0} \quad , \quad \frac{dw}{dx} = -\frac{dw^M}{dx} = 0 \qquad (8)$$

This condition yields to

$$C_1 = C_2 = -\frac{a^2 p}{2Et} \qquad (9)$$

Provided that the thickness of the shell is divided into n layers as shown in Figure 8-b, the parameters in eq.s (6) and (7) become

$$t = \frac{t_0}{n} \quad , \quad \kappa = \sqrt[4]{3(1-\nu^2)}\sqrt{\frac{na}{t_0}} \qquad (10)$$

The boundary conditions in eq. (8) hold as the membrane deformation remains the same.

From these relations, the bending moment of the n-layered shell end is derived as follows:

$$M_x|_{\xi=0} = -\frac{2D\kappa^2}{a^2} C_1 = \frac{a t_0 p}{2\sqrt{3(1-\nu^2)}} \frac{1}{n^2} \qquad (11)$$

Dividing eq. (11) by $Z = \frac{t^2}{6} = \frac{t_0^2}{6n^2}$, we have

$$\sigma_{x,\max} = \sqrt{\frac{3}{1-\nu^2}} \frac{ap}{t_0} \qquad (12)$$

On the other hand, the transverse shearing force becomes

$$Q_x|_{\xi=0} = -\frac{Et}{\kappa a} C_1 = \frac{p}{\sqrt[4]{3(1-\nu^2)}}\sqrt{\frac{t_0 a}{n^3}} \qquad (13)$$

Therefore, we have

$$\tau_{xr,\text{mean}} = \frac{Q_x}{t} = \frac{nQ_x}{t_0} = \frac{p}{\sqrt[4]{3(1-\nu^2)}}\sqrt{\frac{a}{nt_0}} \qquad (14)$$

It is obvious from eq.s (12) and (14) that the division of the shell thickness into n layers retains the maximum bending stress unchanged, while it reduces the transverse shearing stress by the factor of $1/\sqrt{n}$ compared to the original single-layered shell. These characteristics can be clearly observed in the actual stress distribution in the examples shown in Figure 8-a.

It must be noted that the same kind of reduction of the shearing stress is anticipated also in the case of thermal loadings in which the expansion of the cylinder is constrained by the base mat.

4. Ultimate Strength of the Composite Containment Shell

The most important characteristics in the design of containments are the ultimate strength against the inner pressure and earthquakes.

In order to investigate the ultimate behavior of the developed containment, a series of analysis and failure tests are under way. Figures 9 amd 10 show a specimen for failure test by hydraulic inner pressure.

REFERENCES

[1] ACI-ASME Committee 359. "Code for Concrete Reactor Vessels and Containments (ACI359-74)"

[2] L.S.D. Morley, "The Triangular Equilibrium Element in the Solution of Plate Bending Problems.", Aero Quarts., 19, (1968).

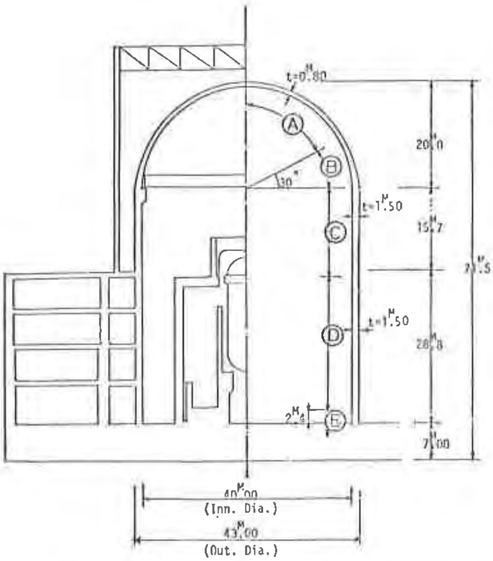

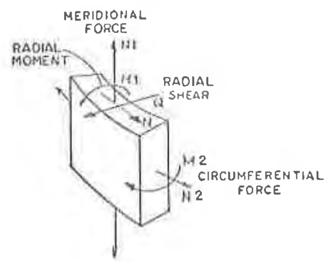

FIG,2 CONTAINMENT WALL FORCES AND MOMENTS

FIG.1 CROSS SECTION OF THE CONTAINMENT WITH COMBINATION BUILDING

TABLE 1- THERMAL CONDITIONS

CONDITION	AMBIENT TEMPERATURE A	B	C	AVERAGE TEMP. CHANGE CASE NO.	DIFFERENTIAL TEMP. CHANGE CASE NO.
WINTER OPERATION	32°C	10°C	0°C	Ta-1	Tg-1
SHUTDOWN	10	10	0	Ta-2	Tg-2
SUMMER OPERATION	32	35	35	Ta-3	Tg-3
SHUTDOWN	30	35	35	Ta-4	Tg-4
WINTER ACCIDENT	85	10	0	Ta-5	Tg-5
SUMMER ACCIDENT	85	35	35	Ta-6	Tg-6
WINTER ACCIDENT (TRANSIENT)	85	10	0	Ta-7	Tg-7

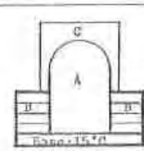

TABLE 2- LOAD CONBINATIONS

Case No.	D+L	F	Pt	Pa	Tt	To	Ta	Eo	Ess	Category
1	1.0		1.0							
1'	1.0		1.0		1.0					Test
2	1.0									
2'	1.0					1.0				Normal
3	1.0							1.0		
3'	1.0					1.0		1.0		Severe environmental
4	1.0								1.0	
4'	1.0					1.0			1.0	Extreme environmental
5	1.0			1.0						
5'	1.0			1.0			1.0			Abnormal
6	1.0			1.5						
6'	1.0			1.5			1.0			Abnormal
7	1.0			1.0				1.0		
7'	1.0			1.0			1.0	1.0		
8	1.0			1.0					1.0	
8'	1.0			1.0			1.0		1.0	Abnormal/Extreme environmental

TABLE 3 - THERMAL FORCES AND MOMENTS

(A)

NO	N1 (T/M)	M1 (TM/M)	N2 (T/M)	M2 (TM/M)	Q (T/M)	NO	N1 (T/M)	M1 (TM/M)	N2 (T/M)	M2 (TM/M)	Q (T/M)	NO	N1 (T/M)	M1 (TM/M)	N2 (T/M)	M2 (TM/M)	Q (T/M)
TA1	-0.0	-0.0	-0.0	-0.0	0.0	TG1	6.4	42.2	0.1	49.1	-0.6	TOTAL1	6.4	42.2	0.1	49.1	-0.6
TA2	0.0	0.0	0.0	0.0	-0.0	TG2	2.0	13.2	0.0	15.4	-0.2	TOTAL2	2.0	13.2	0.0	15.4	-0.2
TA3	-0.0	-0.0	-0.0	-0.0	0.0	TG3	-0.6	-4.0	-0.0	-4.6	0.1	TOTAL3	-0.6	-4.0	-0.0	-4.6	0.1
TA4	-0.0	-0.0	-0.0	-0.0	0.0	TG4	-1.0	-6.6	-0.0	-7.7	0.1	TOTAL4	-1.0	-6.6	-0.0	-7.7	0.1
TA5	-0.0	0.0	-0.0	0.0	0.0	TG5	14.5	95.4	0.2	111.0	-1.4	TOTAL5	14.4	95.4	0.2	111.1	-1.4
TA6	-0.0	0.0	-0.0	0.0	0.0	TG6	7.5	49.5	0.1	57.6	-0.7	TOTAL6	7.5	49.5	0.1	57.6	-0.7
TA7	-0.0	0.0	-0.0	0.0	0.0	TG7	13.4	88.8	0.1	103.4	-1.3	TOTAL7	13.4	88.8	0.1	103.4	-1.3

(B)

NO	N1 (T/M)	M1 (TM/M)	N2 (T/M)	M2 (TM/M)	Q (T/M)	NO	N1 (T/M)	M1 (TM/M)	N2 (T/M)	M2 (TM/M)	Q (T/M)	NO	N1 (T/M)	M1 (TM/M)	N2 (T/M)	M2 (TM/M)	Q (T/M)
TA1	0.0	0.0	-0.0	0.0	-0.0	TG1	-0.5	46.0	0.2	46.8	0.3	TOTAL1	-0.5	46.0	0.2	46.8	0.3
TA2	-0.0	-0.0	-0.0	-0.0	0.0	TG2	-0.2	14.4	0.1	14.6	0.1	TOTAL2	-0.2	14.4	0.0	14.6	0.1
TA3	0.0	0.0	0.0	0.0	-0.0	TG3	0.0	-4.3	-0.0	-4.4	-0.0	TOTAL3	0.1	-4.3	0.0	-4.4	-0.0
TA4	0.0	0.0	0.0	0.0	-0.0	TG4	0.1	-7.2	-0.0	-7.3	-0.1	TOTAL4	0.1	-7.2	-0.0	-7.3	-0.1
TA5	0.1	0.0	1.2	-0.0	-0.1	TG5	-1.1	104.1	0.5	105.8	0.8	TOTAL5	-1.0	104.1	1.7	105.8	0.7
TA6	0.1	0.0	1.1	-0.0	-0.1	TG6	-0.6	54.0	0.3	54.9	0.4	TOTAL6	-0.4	54.0	1.4	54.9	0.3
TA7	0.1	0.0	0.9	-0.0	-0.1	TG7	-0.8	97.3	0.8	98.6	0.5	TOTAL7	-0.7	97.3	1.7	98.6	0.5

(C)

NO	N1 (T/M)	M1 (TM/M)	N2 (T/M)	M2 (TM/M)	Q (T/M)	NO	N1 (T/M)	M1 (TM/M)	N2 (T/M)	M2 (TM/M)	Q (T/M)	NO	N1 (T/M)	M1 (TM/M)	N2 (T/M)	M2 (TM/M)	Q (T/M)
TA1	-0.0	-15.1	-1.8	-2.5	3.7	TG1	-0.0	143.4	-4.3	161.9	6.0	TOTAL1	-0.0	128.3	-6.1	159.4	9.7
TA2	0.0	48.2	246.9	8.0	-36.7	TG2	-0.0	29.6	-4.6	48.1	5.8	TOTAL2	-0.0	77.7	242.3	56.1	-30.9
TA3	-0.0	-106.4	-418.3	-17.8	68.0	TG3	0.0	-15.5	-0.0	-15.5	-0.0	TOTAL3	-0.0	-122.0	-418.4	-33.3	67.9
TA4	-0.0	-100.7	-395.7	-16.8	64.3	TG4	0.0	-25.0	-0.3	-25.7	-0.2	TOTAL4	0.0	-125.7	-396.1	-42.6	64.1
TA5	-0.0	-85.3	-291.4	-14.2	50.0	TG5	-0.0	357.9	-8.8	365.1	3.6	TOTAL5	-0.0	272.6	-300.3	350.9	53.6
TA6	-0.0	-174.3	-687.6	-29.1	111.7	TG6	-0.0	187.8	0.5	187.9	0.3	TOTAL6	-0.0	13.5	-687.1	158.8	112.0
TA7	-0.0	-37.0	-87.4	-6.2	17.7	TG7	-0.0	247.7	-3.9	265.6	5.8	TOTAL7	-0.0	210.8	-91.3	259.4	23.5

(D)

NO	N1 (T/M)	M1 (TM/M)	N2 (T/M)	M2 (TM/M)	Q (T/M)	NO	N1 (T/M)	M1 (TM/M)	N2 (T/M)	M2 (TM/M)	Q (T/M)	NO	N1 (T/M)	M1 (TM/M)	N2 (T/M)	M2 (TM/M)	Q (T/M)
TA1	-0.0	-24.7	-154.7	-4.1	22.9	TG1	-0.0	113.3	-0.2	113.8	-0.5	TOTAL1	-0.0	88.5	-154.9	109.7	22.4
TA2	0.0	19.1	130.0	3.2	-18.8	TG2	-0.0	-0.6	-0.2	-0.1	-0.5	TOTAL2	-0.0	18.5	129.8	3.1	-19.2
TA3	-0.0	-73.7	-478.8	-12.3	70.1	TG3	0.0	-15.5	0.0	-15.5	0.0	TOTAL3	-0.0	-89.2	-478.8	-27.8	70.1
TA4	-0.0	-69.7	-452.9	-11.6	66.3	TG4	0.0	-24.8	-0.2	-25.7	-0.1	TOTAL4	0.0	-94.5	-453.1	-37.3	66.2
TA5	-0.0	-70.4	-452.5	-11.8	66.4	TG5	-0.0	316.4	-0.1	317.2	-0.5	TOTAL5	-0.0	246.0	-452.6	305.4	65.9
TA6	-0.0	-121.1	-786.8	-20.2	115.2	TG6	-0.0	187.9	-0.0	187.9	-0.0	TOTAL6	-0.0	66.8	-786.8	167.7	115.2
TA7	-0.0	-40.3	-255.6	-6.7	37.7	TG7	-0.0	218.9	-0.2	219.4	-0.4	TOTAL7	-0.0	178.6	-255.9	212.7	37.2

(E)

NO	N1 (T/M)	M1 (TM/M)	N2 (T/M)	M2 (TM/M)	Q (T/M)	NO	N1 (T/M)	M1 (TM/M)	N2 (T/M)	M2 (TM/M)	Q (T/M)	NO	N1 (T/M)	M1 (TM/M)	N2 (T/M)	M2 (TM/M)	Q (T/M)
TA1	-0.0	-56.4	-207.0	-9.4	37.3	TG1	-0.0	113.9	-0.0	113.9	0.0	TOTAL1	-0.0	57.5	-207.0	104.5	37.3
TA2	0.0	46.9	172.5	7.8	-31.0	TG2	-0.0	-0.0	-0.0	-0.0	0.0	TOTAL2	-0.0	46.9	172.5	7.8	-31.0
TA3	-0.0	-173.7	-638.3	-29.0	115.0	TG3	0.0	-15.5	0.0	-15.5	0.0	TOTAL3	-0.0	-189.2	-638.3	-44.5	115.0
TA4	-0.0	-164.3	-603.8	-27.4	108.7	TG4	0.0	-26.3	0.0	-26.0	0.2	TOTAL4	0.0	-190.6	-603.7	-53.4	108.9
TA5	-0.0	-164.3	-603.6	-27.4	108.8	TG5	-0.0	317.3	-0.0	317.3	0.0	TOTAL5	-0.0	153.0	-603.8	289.9	108.8
TA6	-0.0	-285.4	-1048.0	-47.7	188.9	TG6	-0.0	187.9	-0.0	187.9	-0.0	TOTAL6	-0.0	-97.4	-1048.8	140.3	188.9
TA7	-0.0	-93.0	-341.6	-15.5	61.5	TG7	-0.0	219.5	-0.0	219.5	0.0	TOTAL7	-0.0	126.5	-341.6	204.0	61.5

TABLE 4 – COMBINED FORCES AND MOMENTS

	CASE NO	N1 (T/M)	M1 (TM/M)	N2 (T/M)	M2 (TM/M)	Q (T/M)	N (T/M)	CASE NO	N1 (T/M)	M1 (TM/M)	N2 (T/M)	M2 (TM/M)	Q (T/M)	N (T/M)
A	1	91.0	-0.8	107.9	-0.4	2.7	0.0	1*	97.5	41.4	108.0	48.7	2.1	0.0
	2	-19.0	-0.1	-21.9	-0.3	-0.6	0.0	2*	-12.5	42.1	-21.8	48.9	-1.2	0.0
	3	10.8	13.2	13.2	12.9	-17.1	-9.7	3*	17.2	55.4	13.3	62.0	-17.7	-9.7
	4	23.3	19.9	28.0	19.4	-25.4	-14.5	4*	29.8	62.1	28.1	68.6	-26.0	-14.5
	5	76.7	-0.8	91.0	-0.4	2.3	0.0	5*	91.1	94.6	91.1	110.6	0.9	0.0
	6	124.5	-1.1	147.4	-0.5	3.7	0.0	6*	139.0	94.3	147.5	110.6	2.3	0.0
	7	106.4	12.6	126.0	12.7	-14.2	-9.7	7*	120.9	108.0	126.1	123.8	-15.6	-9.7
	8	119.0	19.3	140.9	19.3	-22.5	-14.5	8*	133.4	114.7	141.0	130.3	-23.9	-14.5
	CASE NO	N1 (T/M)	M1 (TM/M)	N2 (T/M)	M2 (TM/M)	Q (T/M)	N (T/M)	CASE NO	N1 (T/M)	M1 (TM/M)	N2 (T/M)	M2 (TM/M)	Q (T/M)	N (T/M)
B	1	98.8	-5.4	114.9	-1.1	8.5	0.0	1*	98.3	40.7	115.1	45.7	8.9	0.0
	2	-23.6	1.0	-8.2	-0.0	-2.1	0.0	2*	-24.1	47.1	-8.0	46.8	-1.8	0.0
	3	4.0	-1.0	-85.4	-0.6	-3.2	48.2	3*	3.5	45.0	-85.1	46.2	-2.8	48.2
	4	14.9	-1.9	-124.9	-1.0	-4.0	72.3	4*	14.4	44.2	-124.7	45.9	-3.6	72.3
	5	82.8	-4.5	98.8	-1.0	7.1	0.0	5*	81.9	99.6	100.5	104.8	7.8	0.0
	6	136.0	-7.3	152.4	-1.4	11.8	0.0	6*	135.1	96.8	154.1	104.4	12.4	0.0
	7	110.4	-6.5	21.7	-1.6	6.1	48.2	7*	109.5	97.5	23.4	104.2	6.7	48.2
	8	121.4	-7.4	-17.9	-1.9	5.3	72.3	8*	120.4	96.7	-16.2	103.9	6.0	72.3
	CASE NO	N1 (T/M)	M1 (TM/M)	N2 (T/M)	M2 (TM/M)	Q (T/M)	N (T/M)	CASE NO	N1 (T/M)	M1 (TM/M)	N2 (T/M)	M2 (TM/M)	Q (T/M)	N (T/M)
C	1	10.0	-41.6	88.0	-6.9	26.7	0.0	1*	10.0	86.7	81.9	152.5	36.5	0.0
	2	-115.1	-2.9	-12.9	-0.5	1.8	0.0	2*	-115.1	125.4	-19.0	158.9	11.5	0.0
	3	386.7	71.7	114.2	12.4	43.7	386.9	3*	386.7	199.9	108.1	171.8	53.4	386.9
	4	623.7	108.6	176.1	18.7	64.8	580.3	4*	623.7	236.9	170.0	178.2	74.5	580.3
	5	-6.3	-36.6	74.8	-6.1	23.5	0.0	5*	-6.3	236.1	-225.5	344.7	77.1	0.0
	6	48.1	-53.4	118.7	-8.9	34.3	0.0	6*	48.1	219.2	-181.6	341.9	88.0	0.0
	7	495.5	38.0	201.9	6.8	65.3	386.9	7*	495.5	310.6	-98.4	357.6	119.0	386.9
	8	732.6	75.0	263.9	13.1	86.5	580.3	8*	732.6	347.6	-36.4	364.0	140.1	580.3
	CASE NO	N1 (T/M)	M1 (TM/M)	N2 (T/M)	M2 (TM/M)	Q (T/M)	N (T/M)	CASE NO	N1 (T/M)	M1 (TM/M)	N2 (T/M)	M2 (TM/M)	Q (T/M)	N (T/M)
D	1	-49.4	-30.2	56.6	-5.0	28.4	0.0	1*	-49.4	58.3	-98.4	104.6	98.5	0.0
	2	-174.5	-3.7	-21.7	-0.6	3.2	0.0	2*	-174.5	84.8	-176.6	109.0	73.3	0.0
	3	534.6	6.9	5.7	0.3	13.2	239.8	3*	534.6	95.4	-149.3	110.0	83.3	239.8
	4	868.2	11.7	16.8	0.7	18.6	359.7	4*	868.2	100.3	-138.2	110.4	88.7	359.7
	5	-65.7	-26.7	46.4	-4.5	25.1	0.0	5*	-65.7	219.3	-406.2	301.0	140.3	0.0
	6	-11.3	-38.3	80.4	-6.4	36.1	0.0	6*	-11.3	207.8	-372.2	299.1	151.2	0.0
	7	643.4	-16.2	73.7	-3.5	35.2	239.8	7*	643.4	229.9	-378.9	301.9	150.3	239.8
	8	977.0	-11.3	84.8	-3.1	40.6	359.7	8*	977.0	234.7	-367.8	302.3	155.7	359.7
	CASE NO	N1 (T/M)	M1 (TM/M)	N2 (T/M)	M2 (TM/M)	Q (T/M)	N (T/M)	CASE NO	N1 (T/M)	M1 (TM/M)	N2 (T/M)	M2 (TM/M)	Q (T/M)	N (T/M)
E	1	-140.8	-74.1	-23.5	-12.4	49.2	0.0	1*	-140.8	-16.6	-230.5	92.1	164.2	0.0
	2	-265.9	-11.7	-44.4	-1.9	7.8	0.0	2*	-265.9	45.9	-251.4	102.5	122.8	0.0
	3	621.8	129.0	103.8	21.5	55.2	228.7	3*	621.8	186.5	-103.2	126.0	170.1	228.7
	4	1033.7	197.9	172.6	33.1	79.8	343.0	4*	1033.7	255.4	-34.4	137.5	194.7	343.0
	5	-157.1	-66.0	-26.2	-11.0	43.8	0.0	5*	-157.1	87.0	-630.0	278.9	232.7	0.0
	6	-102.7	-93.2	-17.2	-15.6	61.8	0.0	6*	-102.7	59.8	-620.9	274.4	250.7	0.0
	7	730.6	74.7	122.0	12.5	91.1	228.7	7*	730.6	227.7	-481.7	302.4	280.0	228.7
	8	1142.5	143.6	190.8	24.0	115.7	343.0	8*	1142.5	296.6	-412.9	313.9	304.6	343.0

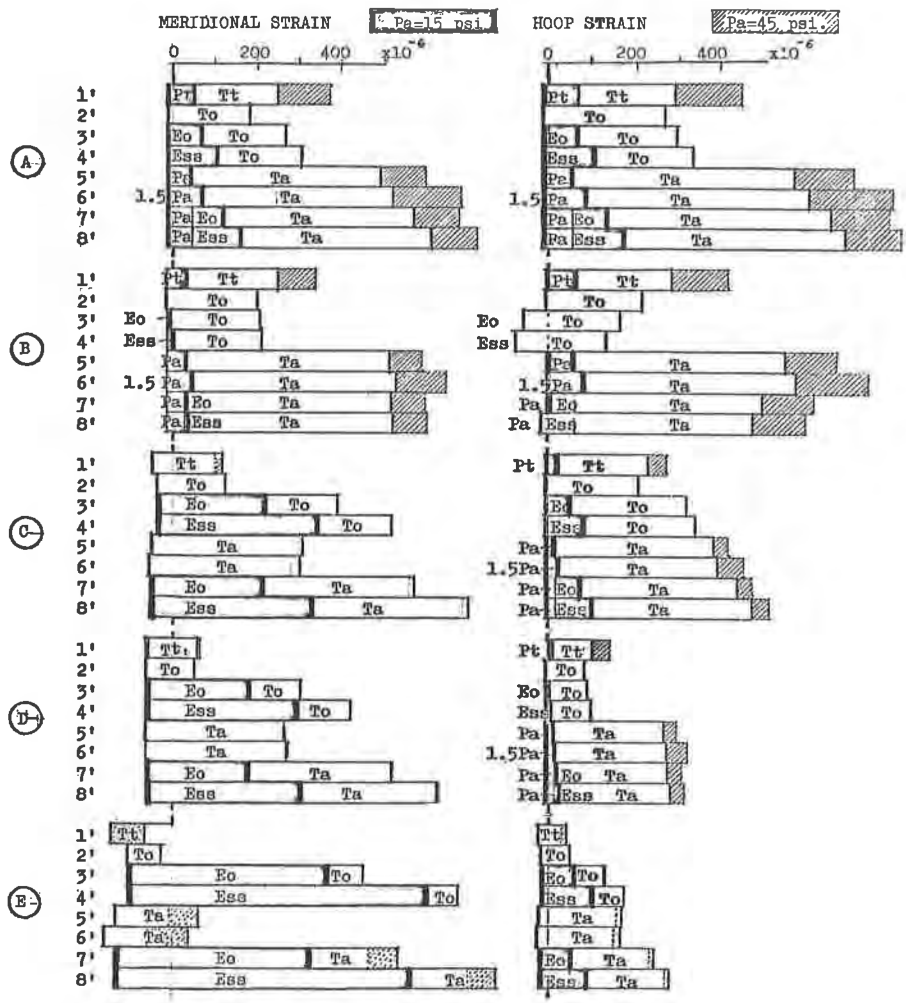

FIG.3 TENSILE STRAIN AT EACH POSITION

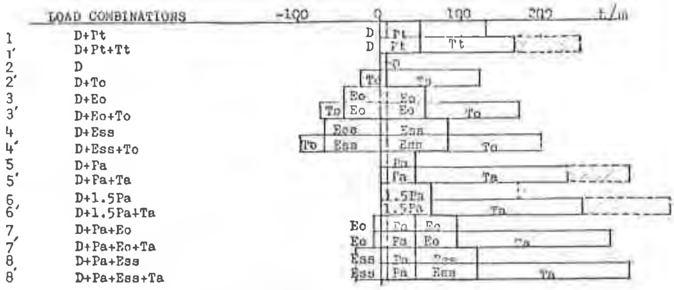

FIG.4 RADIAL SHEAR FORCES AT THE WALL BASE

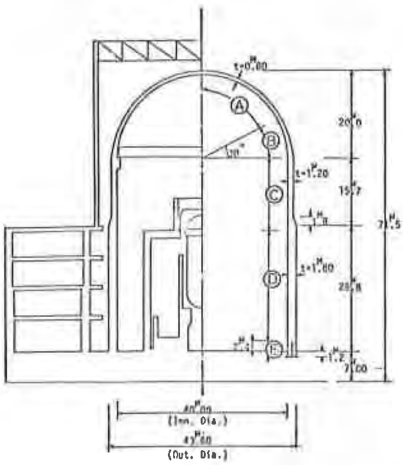

FIG.5 CROSS SECTION OF THE FREE STANDING CONTAINMENT

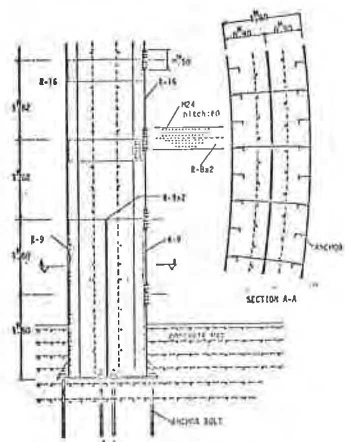

FIG.6-a DETAIL OF THE WALL END

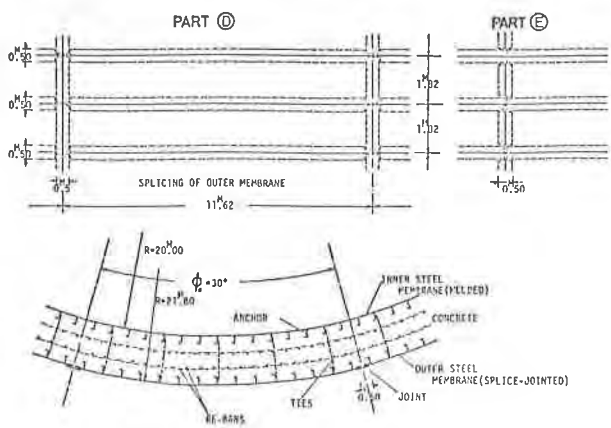

FIG.6-b DETAIL OF THE BARREL WALL

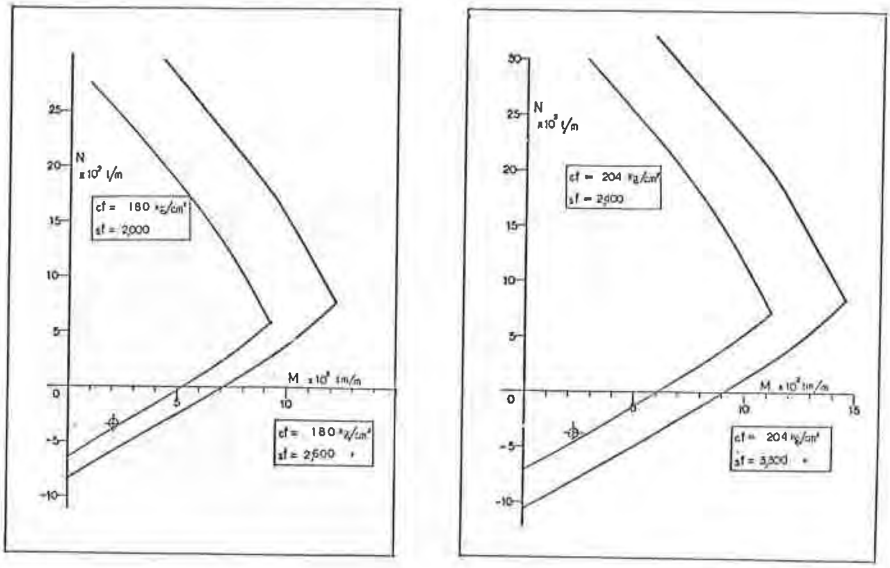

FIG.7 N-M INTERACTION CURVES OF THE STEEL-CONCRETE COMPOSITE SECTION

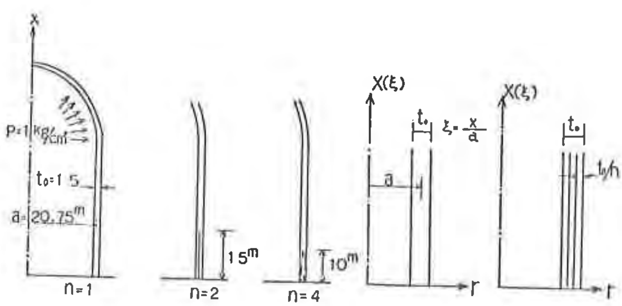

FIG.8-b DIMENSIONS OF THE WALL ENDS

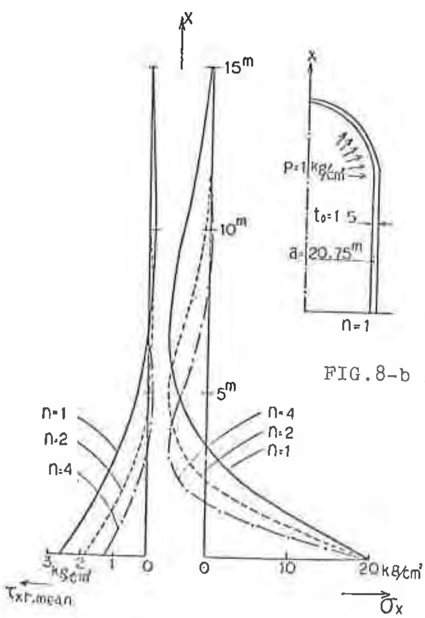

FIG.8-a COMPARISON OF THE WALL END MOMENTS AND SHEARS

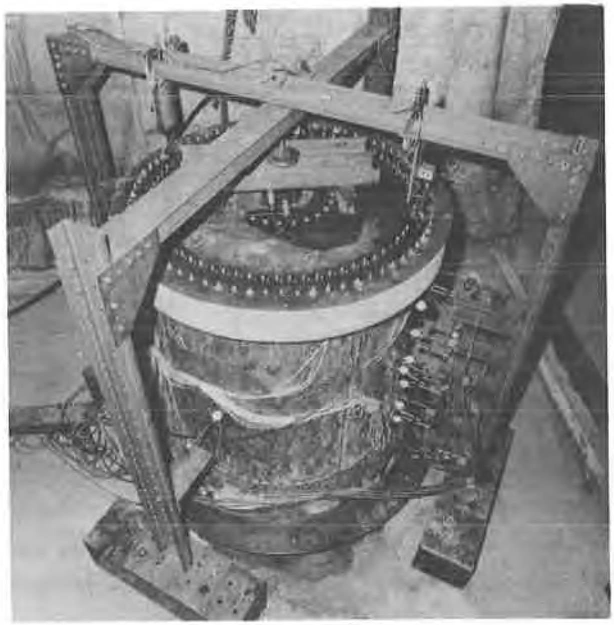

FIG.9 SPECIMEN

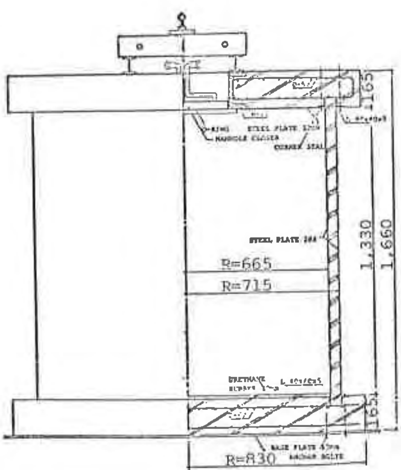

FIG.10 SPECIMEN,SECTIONED DIAGRAM